Promising Fast Energy Transfer System via an Easy Synthesis: Bodipy−Porphyrin Dyads Connected via a Cyanuric Chloride Bridge, Their Synthesis, and Electrochemical and Photophysical...

ARTICLE *in* INORGANIC CHEMISTRY · AUGUST 2011

Impact Factor: 4.76 · DOI: 10.1021/ic201052k · Source: PubMed

9 AUTHORS, INCLUDING:

Theodore Lazarides
Aristotle University of Thessaloniki
35 PUBLICATIONS **1,180** CITATIONS
SEE PROFILE

Marius Réglier
French National Centre for Scientific Research
103 PUBLICATIONS **1,315** CITATIONS
SEE PROFILE

Emmanuel Klontzas
University of Crete
25 PUBLICATIONS **702** CITATIONS
SEE PROFILE

Thanassis Coutsolelos
University of Crete
124 PUBLICATIONS **1,383** CITATIONS
SEE PROFILE

Inorganic Chemistry

ARTICLE

pubs.acs.org/IC

Promising Fast Energy Transfer System via an Easy Synthesis: Bodipy−Porphyrin Dyads Connected via a Cyanuric Chloride Bridge, Their Synthesis, and Electrochemical and Photophysical Investigations[⊥]

Theodore Lazarides,[†] Georgios Charalambidis,[†] Alexandra Vuillamy,[†,§] Marius Réglier,[*,§] Emmanuel Klontzas,[†] Georgios Froudakis,[†] Susanne Kuhri,[‡] Dirk M. Guldi,[*,‡] and Athanassios G. Coutsolelos[*,†]

[†]Laboratory of Bioinorganic Chemistry, Chemistry Department, University of Crete, Voutes Campus, P.O. Box 2208, 71003 Heraklion, Crete, Greece

[‡]Department of Chemistry and Pharmacy, Interdisciplinary Center for Molecular Materials (ICMM), Friedrich-Alexander-Universitaet of Erlangen-Nuernberg, Egerlandstrasse 3, 91058 Erlangen, Germany

[§]ISM2 UMR 6263, CNRS, Aix-Marseille Université, 13397 Marseille, Cedex 20, France

Supporting Information

ABSTRACT: The boron dipyrrin (Bodipy) chromophore was combined with either a free-base or a Zn porphyrin moiety (H_2P and ZnP respectively), via an easy synthesis involving a cyanuric chloride bridging unit, yielding dyads Bodipy-H_2P (**4**) and Bodipy-ZnP (**5**). The photophysical properties of Bodipy-H_2P (**4**) and Bodipy-ZnP (**5**) were investigated by UV-Vis absorption and emission spectroscopy, cyclic voltammetry, and femtosecond transient absorption spectroscopy. The comparison of the absorption spectra and cyclic voltammograms of dyads Bodipy-H_2P (**4**) and Bodipy-ZnP (**5**) with those of their model compounds Bodipy, H_2P, and ZnP shows that the spectroscopic and electrochemical properties of the constituent chromophores are essentially retained in the dyads indicating negligible interaction between them in the ground state. In addition, luminescence and transient absorption experiments show that excitation of the Bodipy unit in Bodipy-H_2P (**4**) and Bodipy−ZnP (**5**) into its first singlet excited state results in rapid Bodipy to porphyrin energy transfer—$k_4 = 2.9 \times 10^{10}$ s^{-1} and $k_5 = 2.2 \times 10^{10}$ s^{-1} for Bodipy-H_2P (**4**) and Bodipy-ZnP (**5**), respectively-generating the first porphyrin-based singlet excited state. The porphyrin-based singlet excited states give rise to fluorescence or undergo intersystem crossing to the corresponding triplet excited states. The title complexes could also be used as precursors for further substitution on the third chlorine atom on the cyanuric acid moiety.

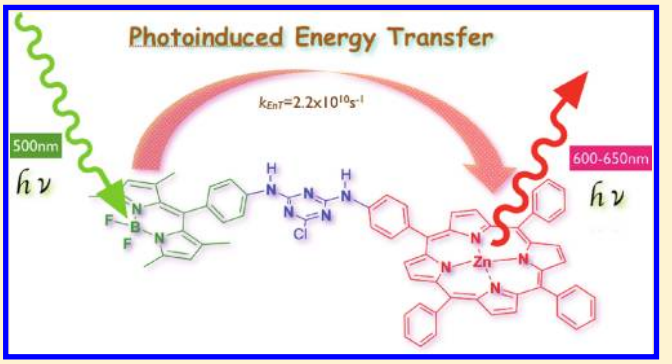

INTRODUCTION

Molecular systems combining two or more chromophores have enjoyed continuing interest in their photophysical and photochemical properties due to their potential for important applications ranging from light harvesting and storage to sensors and optoelectronic devices.[1−3] Recent developments in the field of dye-sensitized solar cells (DSSCs) have shown that porphyrin derivatives are good candidates for photovoltaic applications due to their highly reducing excited state which leads to efficient electron injection into metal oxide semiconductors such as ZnO or TiO_2.[4−6] However, despite the favorable excited state redox potentials of porphyrins, their relatively modest molar absorptivity values in the low-energy visible region (maximum ε of ~20 000 M^{-1} cm^{-1} at 500−700 nm)[7] represent a significant drawback for their use in photocurrent generation. To improve their light-harvesting potential, porphyrins can be derivatized with highly absorbing antenna chromophores, which act as sensitizers of the porphyrin-based excited state. The boron dipyrrin, Bodipy, chromophore is particularly effective as an antenna group for porphyrins and phthalocyanines as it combines a high fluorescence quantum yield, a relatively long lifetime, a suitable excited state energy, and excellent photostability.[8] A Bodipy−porphyrin conjugate, with an acetylide group as bridge, has recently shown improved power conversion efficiency, η, compared to its parent porphyrin chromophore when used as a sensitizer in a DSSC.[9] In search of alternative ways to combine Bodipy and porphyrin chromophores we explored the

Received: May 18, 2011
Published: August 16, 2011

Scheme 1. Synthesis of the Compounds Discussed in This Paper (1−5)

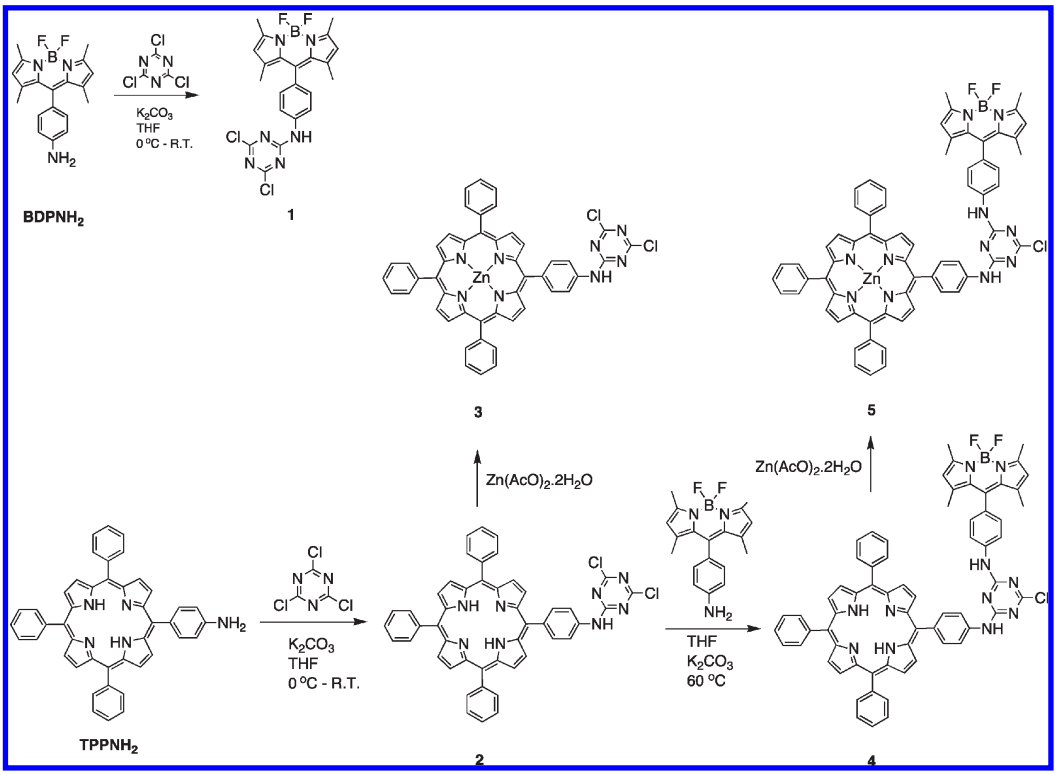

use of cyanuric chloride as a bridging unit. Cyanuric chloride has been used as the linker for the preparation of porphyrinic dimers and oligomers[10−12] and porphyrin−oxadiazole dyads[13] and for the immobilization of porphyrins on resin beads.[14] In this work, we describe the facile synthesis of Bodipy−porphyrin dyads using cyanuric chloride as the linker. The dyads are studied photophysically by steady state and time-resolved absorption and emission spectroscopy to investigate the dynamics and mechanism of Bodipy to porphyrin energy transfer, which are discussed along with the potential importance of such dyads as sensitizers in solar energy conversion schemes.

RESULTS AND DISCUSSION

Synthesis and Characterization. The synthesis of the compounds discussed in this paper is shown in Scheme 1. Reaction of **BDPNH$_2$** with cyanuric chloride under low-temperature conditions (0 °C to room temperature) affords the monoadduct **1**, which is stable enough to be purified by column chromatography. Similarly, reaction of **TPPNH$_2$** with cyanuric chloride leads to the precursor **2**,[11,27] which can be readily converted to the corresponding Zn complex, **3**, by treatment with Zn(CH$_3$COO)$_2$·2H$_2$O. The Bodipy−porphyrin conjugate **4** can be obtained by reaction of **2** with **BDPNH$_2$** at 60 °C. At this higher temperature, the second chloride of the cyanuric chloride group can be substituted by an amine.[11] Reaction of the free base porphyrin derivative **4** with Zn(CH$_3$COO)$_2$·2H$_2$O readily affords the corresponding Zn derivative **5**. The new compounds **1**−**5** were characterized on the basis of their ^{1}H and ^{13}C NMR spectra, MALDI-TOF mass spectra, and elemental analyses. Further details on their synthesis and characterization can be found in the Experimental Section.

NMR Spectroscopy. Confirmation of the molecular formulas from the coupling of the cyanuric chloride on the monoamino porphyrin to the final derivatives metalated with zinc or not has been followed by ^{1}H NMR and ^{13}C NMR experiments. There is no significant chemical shift displacement observed during the transformations with respect to the used starting materials. Figure 1 depicts the proton NMR spectra of compounds **4** and **5**. However, except the presence of all protons for each entity, several chemical shifts of the key protons in the different steps have been observed. The presence of the cyanuric group between the monoamino porphyrin and the amino Bodipy could be confirmed by the displacement of the chemical shift of the phenyl group protons at higher frequencies. Attachment of the Bodipy influences its pyrrolic protons: from a singlet corresponding to two protons, two singlet peaks have been observed (see Supporting Information). Finally, after the metalation reaction the peak at −2.76 ppm, which corresponds to the two free protons of the porphyrin ring, disappears.

Electrochemistry. The electrochemical properties of the two Bodipy−porphyrin conjugates, **4** and **5**, and their model compounds, **1**, **2**, and **3**, were investigated by cyclic and square wave voltammetry in dichloromethane. The redox data are collected in Table 1, and some representative cyclic voltammograms are depicted in Figure 2. All data are reported vs the ferrocene/ferrocenium couple (Fc/Fc$^+$). Comparison of the cyclic voltammograms of dyads **4** and **5** with those of their model compounds and the electrochemical data of Bodipy[28,29] and porphyrin[7] derivatives reported in the literature shows that the two reversible processes occurring in the range 0.35−0.52 and 0.71−0.76 V vs

dx.doi.org/10.1021/ic201052k |Inorg. Chem. 2011, 50, 8926–8936

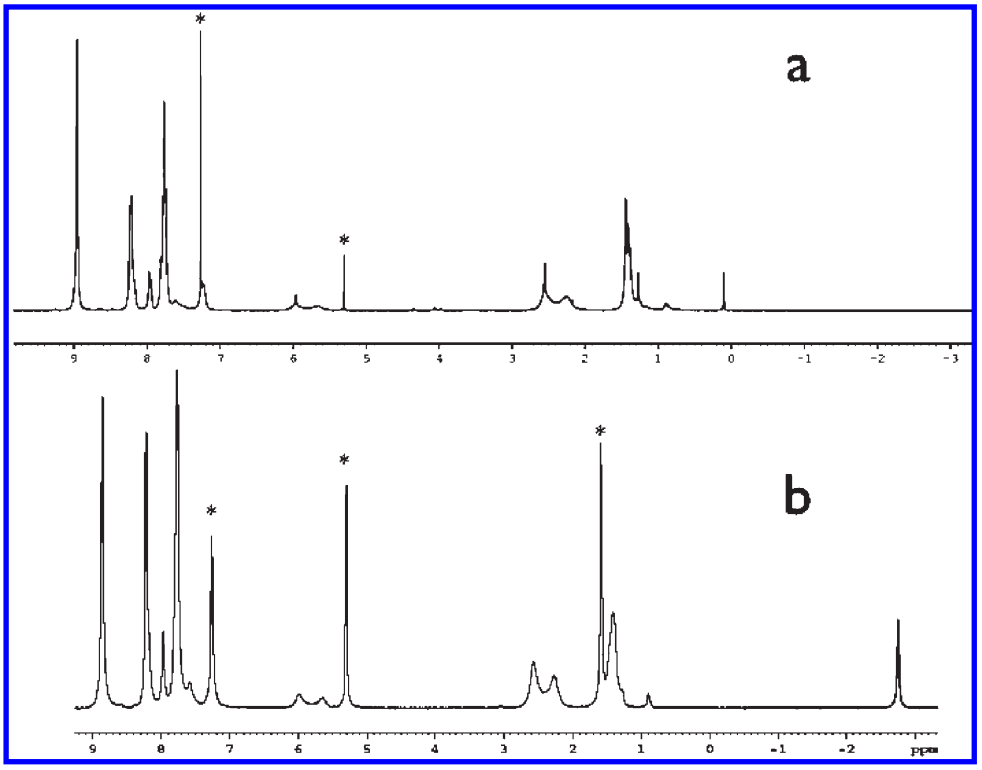

Figure 1. ^{1}H NMR spectrum of **5** (a) and **4** (b). The asterisks (*) denote solvent peaks.

Table 1. Redox Data Reported vs Fc/Fc$^+$ in Dichloromethane Using Tetrabutylammonium Hexafluorophosphate 0.1 M as Supporting Electrolyte[a]

compound	$E_{1/2}^{Ox1}$/V (ΔE_p/V)[b]	$E_{1/2}^{Ox2}$/ V	$E_{1/2}^{Red1}$/ V	$E_{1/2}^{Red2}$/ V
2	0.51(0.07)	0.79(0.07)	−1.71(0.07)	−2.07(0.07)
3	0.37(0.07)	0.68(0.07)	−1.82(0.07)	
1	0.76(0.08)		−1.74(0.08)	
4	0.52(0.06)	0.76(0.15)	−1.70(0.08)	−2.09(0.07)
5	0.35(0.06)	0.71(0.11)	−1.65(0.07)	−1.80(0.06)

[a] All reported waves are reversible (ΔE_p of the Fc/Fc$^+$ couple is 0.07 V). [b] The anodic−cathodic peak separations are given in parentheses.

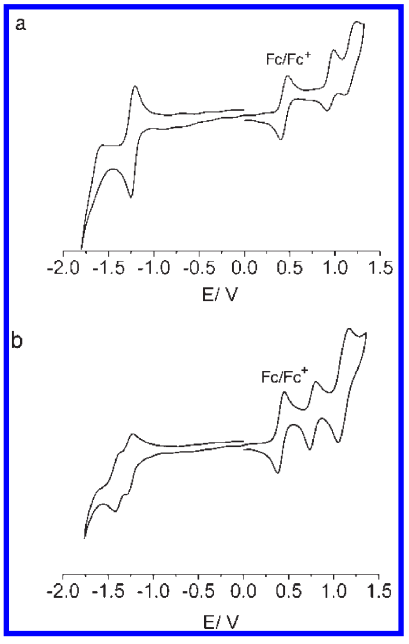

Figure 2. Cyclic voltammograms of a) **3** and b) **5**. The reversible couple of ferrocene (Fc/Fc$^+$) is also shown. The voltages are vs the saturated calomel electrode (SCE).

Fc/Fc$^+$ (Table 1 and Figure 2) are due to the first porphyrin-based oxidation and to the overlapping waves of the second porphyrin and Bodipy-based oxidations, respectively. In addition, the dyad **4** shows two successive reversible processes at −1.70 and −2.09 V vs Fc/Fc$^+$, attributed to the overlapping Bodipy and first porphyrin-based reductions and to the second porphyrin-based reduction, respectively. In **5**, the Bodipy and first porphyrin-based oxidations appear as two closely spaced reversible waves at −1.65 and −1.80 V, respectively. The anticipated second porphyrin-based reduction of **5** is probably obscured due to its occurrence beyond the solvent window,[7] a behavior that is also seen in model compound **3**.

Photophysical Properties. *Electronic Absorption Spectra.* The electronic absorption spectra of **4** and **5** and the model compounds **1**, **2**, and **3** are shown in Figure 3. A collection of absorption data can be found in Table 2. The electronic spectrum of **1** (Figure 3a) is dominated by an intense absorption band at ca. 500 nm attributed to the lowest energy spin-allowed $\pi-\pi^*$ transition of the Bodipy moiety.[30] The spectrum of **1** also shows absorption bands of lower intensity in the 280−380 nm region attributed to higher energy $\pi-\pi^*$ transitions of the Bodipy group.[30] The UV−Vis absorption spectra of **2** and **3** (Figure 3b and 3c), as expected for TPP and ZnTPP-type chromophores, exhibit intense Soret bands at ca. 420 nm and weaker Q bands in

dx.doi.org/10.1021/ic201052k |*Inorg. Chem.* 2011, 50, 8926–8936

the 500−700 nm region (i.e., four Q bands for the free-base porphyrin **4** and two Q bands for the Zn complex **5**).[7]

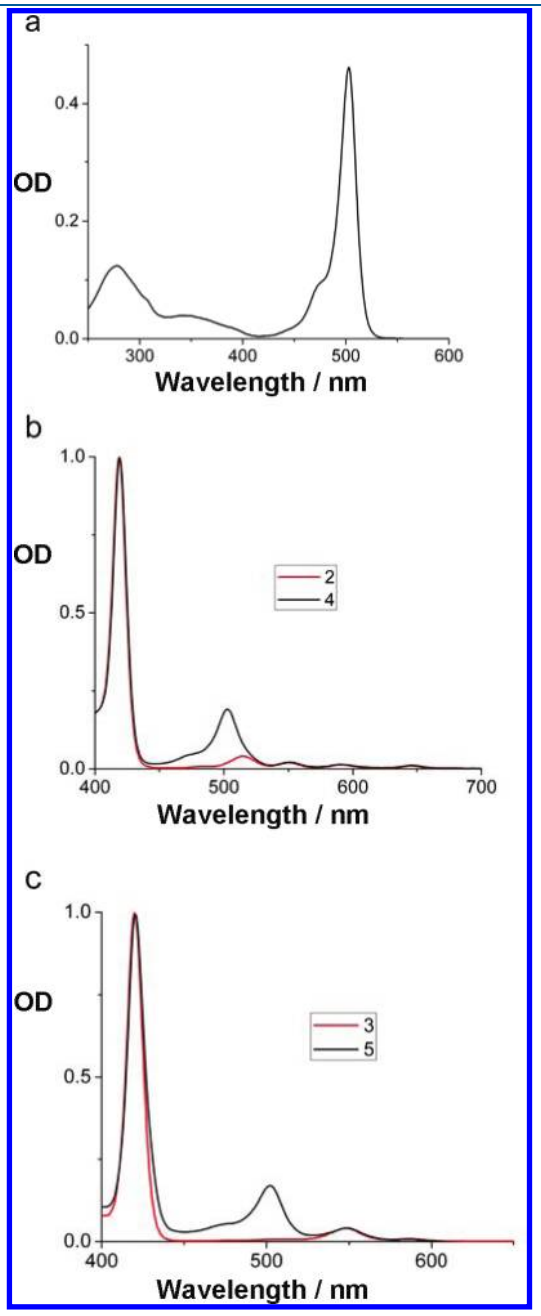

Figure 3. UV−Vis absorption spectra of (a) **1**, (b) **2** and **4** (normalized), and (c) **3** and **5** (normalized) in dichloromethane.

Comparison of the spectra of the dyads **4** and **5** with those of their model compounds **1**, **2**, and **3** shows that they are essentially the sum of their constituent chromophores. This indicates negligible electronic interactions between the porphyrin and Bodipy units in the ground states of the dyads.

Emission Spectra. Compounds **1**−**5** were studied by steady state and time-resolved emission spectroscopy in dichloromethane at ambient temperature. A collection of emission maxima, quantum yields, and lifetimes is given in Table 2. Some representative emission and excitation spectra can be seen in Figures 4 and 5. The Bodipy derivative **1** shows the intense fluorescence of a Bodipy dye[30] at 513 nm with a lifetime, τ_1, of 3.0 ns. The porphyrin derivatives **2** and **3** exhibit the characteristic fluorescence of free-base and Zn porphyrins with emission maxima at 650 and 712 nm for **2** (τ_2 = 8.8 ns) and at 596 and 645 nm for **3** (τ_3 = 1.8 ns). When the dyad **4** is irradiated at 486 nm, corresponding to selective excitation of the Bodipy unit, it shows emission from the porphyrin chromophore at 650 and 714 nm (Figure 4a) in addition to residual fluorescence from the Bodipy group at 512 nm.[30] The Bodipy-based emission in **4** is quenched by ca. 98% when compared to the emission measured for the model compound **1**. In addition, the excitation spectrum of **4** monitoring at the emission of the porphyrin moiety at 652 nm shows a pronounced Bodipy absorption feature at ca. 500 nm (Figure 5a). This is an indication of Bodipy−porphyrin

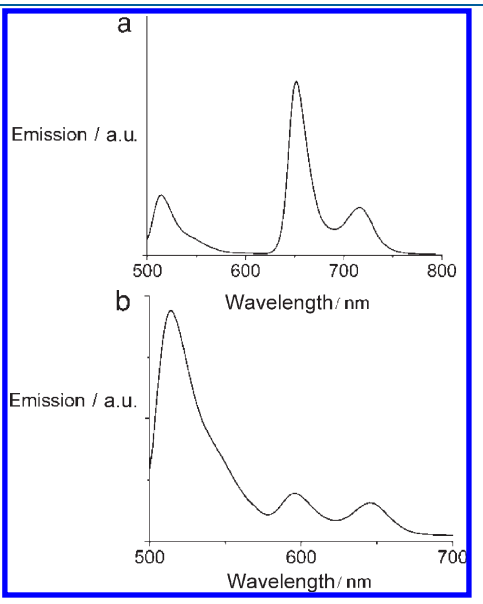

Figure 4. Room temperature emission spectra in dichloromethane of (a) **4** and (b) **5** upon selective excitation of the Bodipy unit at 476 nm.

Table 2. Summary of Spectroscopic Data for Compounds 1−5

	absorption	emission		
compound	λ_{max}/ nm (ε/ $M^{-1}cm^{-1}$)	λ_{max}/ nm	Φ	τ/ ns
1	502(75 600); 342(9400); 277(33 000)	513	0.58	3.0
2	418(478 000); 514(19 000); 549(9000); 589 (6000); 645 (4500)	650; 712	0.11	8.8
3	419(585 000); 542(20 400); 583(6000)	596; 645	0.032	1.8
4	419(419 000); 500(74 800); 550(8300); 589(5200); 645(4200)	512; 650; 714		8.7[a]
5	420(434 000); 500(75 300); 546(21 500); 583(7200)	513; 595; 645		1.9[a]

[a] Measured at the emission wavelengh of a porphyrin moiety using a bandpass filter centered at 670 nm with a bandwidth of ~50 nm.

dx.doi.org/10.1021/ic201052k |*Inorg. Chem.* 2011, 50, 8926–8936

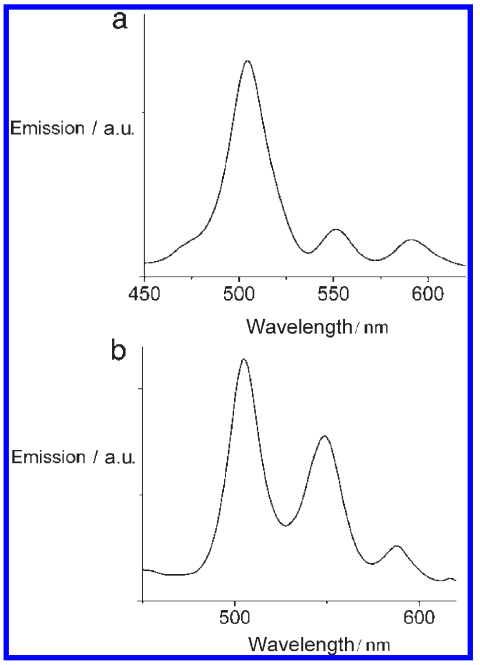

Figure 5. Room temperature excitation spectra of (a) **4** monitoring at 652 nm and (b) **5** monitoring at 654 nm.

energy transfer following excitation of the Bodipy unit. Dyad **5** shows analogous behavior to its nonmetalated counterpart, **4**, as can be seen in the corresponding emission and excitation spectra in Figures 4b and 5b. Excitation of **5** at 486 nm results in dual emission corresponding to the residual fluorescence of the Bodipy unit at ca. 512 nm (quenched by ca. 96% compared to model compound **1**) and to the Zn porphyrin chromophore at 596 and 645 nm. In the case of **5**, the residual Bodipy-based fluorescence is more intense than the sensitized emission of the porphyrin unit. This is mainly due to the intrinsically lower luminescence quantum yield of zinc porphyrins compared to their parent macrocycles.[16] The lifetime of the residual Bodipy-based fluorescence—and therefore the rate of Bodipy to porphyrin energy transfer—in **4** and **5** could not be measured with our experimental setup. However, femtosecond transient absorption measurements discussed below allowed us to analyze the dynamic behavior of **4** and **5** at the picosecond time scale.

Transient Absorption Spectroscopy. Femtosecond transient absorption spectroscopy was used to obtain further insight into the excited state interactions in dyads **4** and **5** and to corroborate the proposed energy transfer process. Toward this end, **1**−**5** were probed with either 420 or 490 nm excitation to excite separately the porphyrin or Bodipy chromophore, respectively.

In the cases of **2** and **3**, the singlet excited states—formed essentially right after the laser pulse—include a net decrease of the absorption around 550 nm, a region which is dominated by the strong free-base porphyrin (H_2P) and Zn porphyrin (ZnP) ground state absorption. This suggests consumption of H_2P and ZnP as a result of converting the singlet ground states of **2** and **3** to the corresponding singlet excited states. An immediately formed absorption accompanies the bleach. For example, the H_2P-based singlet excited state in **2** exhibits a new absorption band between 660 and 730 nm. The singlet transients produced

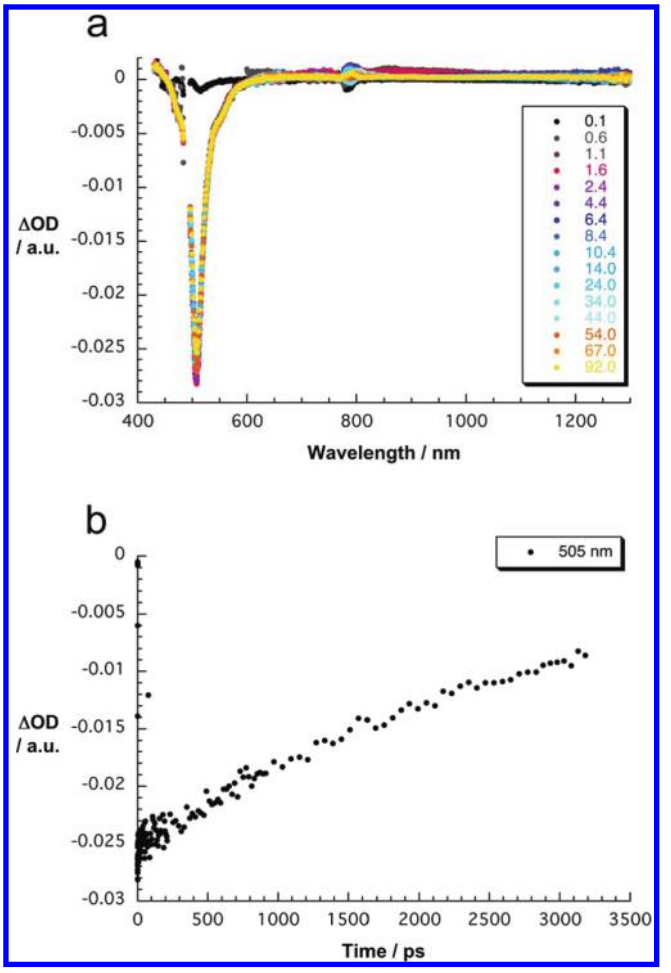

Figure 6. (a) Differential absorption spectra (visible and near-infrared) obtained upon femtosecond flash photolysis (490 nm, 150 nJ) of **1** in toluene with several time delays between 0 and 100 ps at room temperature. (b) Time−absorption profiles of the spectra at 505 nm, monitoring the intersystem crossing dynamics.

upon photoexcitation decay with lifetimes of 9.8 (**2**, H_2P) and 2.1 ns (**3**, ZnP) via intersystem crossing to the corresponding triplet manifold. The main spectral features of the latter state include maxima at 780 (**2**, H_2P) and 840 nm (**3**, ZnP).

The corresponding femtosecond experiments with **1** reveal upon 490 nm laser excitation (Figure 6) the instantaneous formation of the Bodipy-based singlet excited state features. Here, the transient absorption spectra are dominated by a pronounced bleach between 450 and 600 nm, which is due to depletion of the singlet ground state. In the 400 and 700 nm regions additional maxima seem to emerge. Overall, all of the aforementioned Bodipy-based singlet excited state features are long lived (i.e., 3.2 ns). Implicit is a slow intersystem crossing to the corresponding triplet manifold.

The spectral features that are seen immediately (i.e., 1 ps) upon excitation of **5** at 490 nm (Figure 7) are almost superimposable with those recorded for the Bodipy singlet excited state, vide supra. The lifetime of the Bodipy singlet excited state is, however, greatly diminished by the presence of the covalently attached ZnP chromophore. Formation of a new transient develops as a result of the rapid decay (i.e., 45 ps) of the Bodipy-based singlet excited state instead of the much slower

dx.doi.org/10.1021/ic201052k |*Inorg. Chem.* 2011, 50, 8926–8936

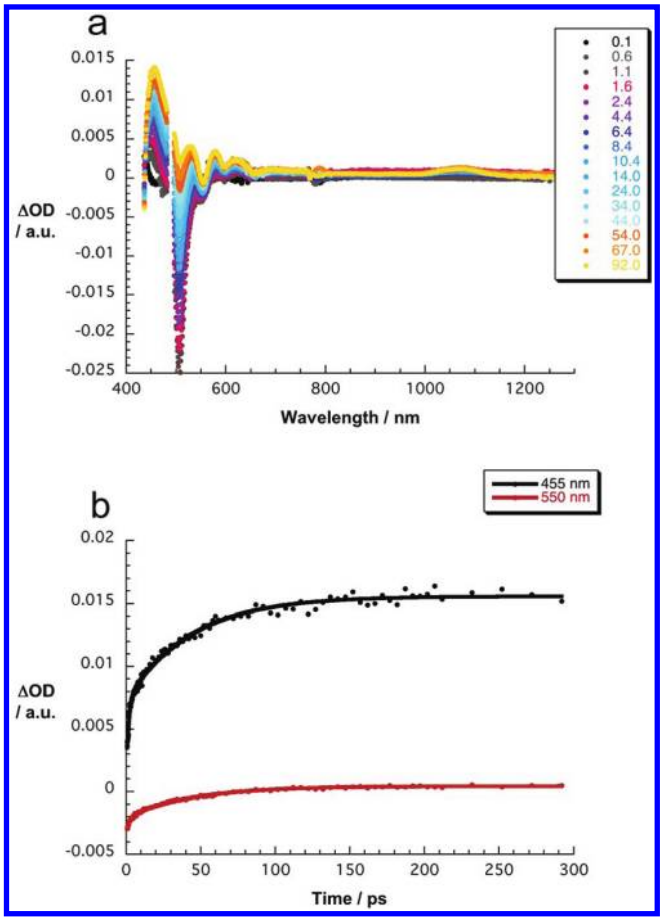

Figure 7. (a) Differential absorption spectra (visible and near-infrared) obtained upon femtosecond flash photolysis (490 nm, 150 nJ) of **5** in toluene with several time delays between 0 and 100 ps at room temperature. (b) Time−absorption profiles of the spectra at 455 and 550 nm, monitoring the intramolecular energy transfer.

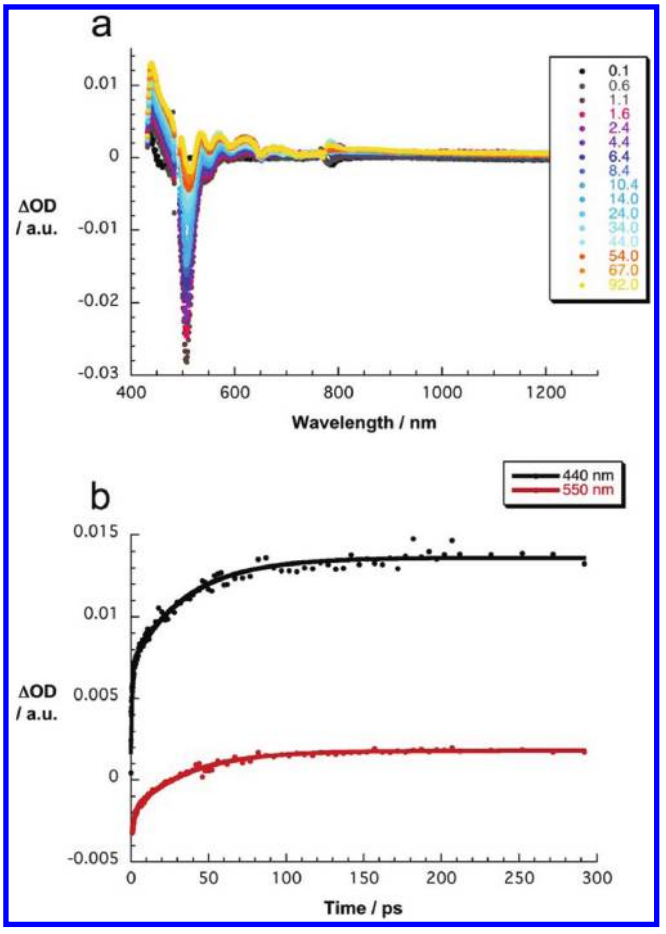

Figure 8. (a) Differential absorption spectra (visible and near-infrared) obtained upon femtosecond flash photolysis (490 nm, 150 nJ) of **4** in toluene with several time delays between 0 and 100 ps at room temperature. (b) Time−absorption profiles of the spectra at 440 and 550 nm, monitoring the intramolecular energy transfer.

intersystem crossing to the triplet excited state. The new transient resembles the singlet excited state characteristics of ZnP, that is, maxima at 455, 580, and 620 nm as well as minima at <430 and 555 nm. This suggests involvement of the ZnP singlet excited state in an intramolecular energy transfer, occurring between the photoexcited Bodipy unit and the singlet ground state of ZnP. The kinetics of Bodipy to porphyrin energy transfer were determined by exponential fitting of the ZnP singlet excited state formation ($k_5 = 2.2 \times 10^{10}$ s^{-1}) as seen in Figure 7. On a longer time scale, the fate of the ZnP-based singlet excited state is identical to that known for Zn porphyrins—intersystem crossing, driven by a strong spin−orbit coupling, governs the transformation (i.e., 2.1 ns) of the singlet into the triplet excited state. The latter was identified by a long-lived (i.e., 100 μs) and strongly absorbing triplet−triplet maximum at 840 nm.

Upon excitation of **4** at 490 nm (Figure 8), the same Bodipy-based singlet excited state features are seen early on (i.e., 1 ps). In line with the photoreactivity of **5**, the Bodipy singlet excited state in **4** decays rapidly (i.e., 34 ps) in the presence of the H_2P chromophore. Importantly, maxima at 440, 570, 620, and 680 nm as well as minima at <430, 550, 590, and 680 nm are exact matches of the H_2P singlet excite state and, in turn, confirm the transduction of singlet excited state energy. The rate constant of energy transfer in **4** is $k_4 = 2.9 \times 10^{10}$ s^{-1}, as shown in Figure 8.

Intersystem crossing is the ultimate fate of the H_2P singlet excited state. However, the correspondingly formed triplet excited state is only discernible on the nanosecond time scale, due to the fact that the intersystem crossing occurs within the 10 ns time window. The most characteristic feature of the H_2P triplet excited state is a 780 nm maximum.

In reference experiments, **4** and **5** were excited at 420 nm. However, due to the dominating H_2P and ZnP-based absorptions at the 420 nm excitation wavelength, no appreciable Bodipy-based features were seen at any time following excitation. Instead, only the H_2P and ZnP characteristics emerge.[31]

In summary, as shown in the Jablonski diagram of Figure 9, excitation of **4** and **5** into their Bodipy-based $\pi-\pi^*$ excited states is followed by energy transfer to the lowest-lying porphyrin-based singlet excited states with rate constants of $k_4 = 2.9 \times 10^{10}$ s^{-1} and $k_5 = 2.2 \times 10^{10}$ s^{-1}, respectively. The slightly faster energy transfer rate measured in dyad **4** correlates well with the larger spectral overlap compared to that in dyad **5**, see discussion below. The observed Bodipy to porphyrin energy transfer rates in **4** and **5** are considerably faster than those measured in other Bodipy−porphyrin dyads with nonconjugated bridges[32] ($\sim 9 \times 10^9$ s^{-1}) and comparable with those found in dyads of this type connected through an amide linkage[8] or a rigid conjugated ethynyl bridge[33] ($\sim 3-5 \times 10^{10}$ s^{-1}).

dx.doi.org/10.1021/ic201052k |*Inorg. Chem.* 2011, 50, 8926–8936

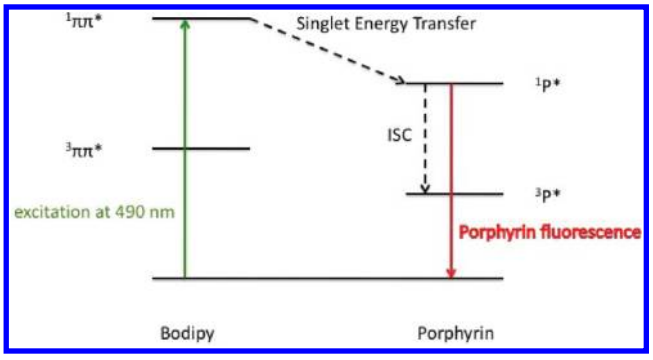

Figure 9. Jablonski diagram relevant to the photophysics of **4** and **5**. $^1P^*$ and $^3P^*$ denote the lowest singlet and triplet porphyrin-based excited states, respectively.

The porphyrin-based singlet excited states formed after Bodipy to porphyrin energy transfer undergo deactivation either to the ground state by radiative decay (fluorescence) or to the corresponding porphyrin-based triplet states by intersystem crossing. The porphyrin-based triplet excited states in **4** and **5** lie, however, lower than the corresponding Bodipy-based triplet excited state, so "back transfer" from the porphyrin to the Bodipy triplet is not possible in these cases. Such "back transfer" was observed in the study of dyads combining a Bodipy chromophore with a Pt^{II}(diimine)(dithiolate) moiety.[34] Thus, the porphyrin-based triplet excited states of **4** and **5** can be readily generated by initial excitation of the Bodipy part of the dyads and could act as effective electron donors in photocurrent or photocatalytic H_2 production schemes.[35]

Discussion on Energy Transfer Mechanism. In general, the mechanism of energy transfer between a donor and an acceptor can be described on the basis of two limiting mechanisms.

(i) A double-electron exchange involving one electron from the LUMO of the excited donor to the empty LUMO of the acceptor with a simultaneous transfer of another electron from the HOMO of the acceptor to the half-filled HOMO of the donor (Dexter mechanism).[36]

(ii) An excitation transfer as a result of dipole−dipole interactions between the energy donor and the acceptor (Förster mechanism).[37]

The rate constant of energy transfer by the Dexter mechanism, k_D, is given by eq 1

$$k_D = \frac{4\pi^2 H^2}{h} J_D \tag{1}$$

where h is Planck's constant, H is the intercomponent electronic interaction parameter, and J_D is the Dexter spectral overlap integral calculated from the area normalized donor emission spectrum, $f_D(\bar{\nu})$, and the area normalized acceptor absorption spectrum expressed by its extinction coefficient, $\varepsilon_A(\bar{\nu})$, both taken on an energy scale, i.e., wavenumbers, $\bar{\nu}$, as shown in eq 2

$$J_D = \int \varepsilon_A(\bar{\nu}) f_D(\bar{\nu}) \mathrm{d}\bar{\nu} \tag{2}$$

The rate constant of energy transfer by the Förster mechanism, k_F, given by eq 3, can be written in terms of the critical transfer radius R_c, which corresponds to the interchromophoric distance at which k_F equals the decay rate of the donor in the absence of an acceptor, τ_D^{-1}

$$k_F = \frac{1}{\tau_D}\left(\frac{R_c}{r}\right)^6 \tag{3}$$

where r is the distance between the two chromophores and R_c is given by eq 4

$$R_c = \left(\frac{9000 \cdot \ln 10 \cdot \kappa^2 \cdot \phi_D}{128 \cdot \pi^5 \cdot N \cdot n^4} J_F\right)^{1/6} \tag{4}$$

where κ^2 is an orientation factor for the two dipoles, ϕ_D is the luminescence quantum yield of the donor, N is Avogadro's number, n is the refractive index of the solvent, and

$$J_F = \int \frac{\varepsilon_A(\bar{\nu}) f_D(\bar{\nu})}{\bar{\nu}^4} \mathrm{d}\bar{\nu} \tag{5}$$

is the Förster spectral overlap integral calculated from the area normalized emission spectrum of the donor, $f_D(\bar{\nu})$, and the absorption spectrum of the acceptor, $\varepsilon_A(\bar{\nu})$.

Regarding the possibility of through-bond Dexter-type[36] Bodipy to porphyrin energy transfer in **4** and **5**, it should be investigated if the bridging unit can effectively mediate orbital interactions between the two chromophores.[38] As can be seen in Figure 10, the results of a DFT calculation on a geometrically optimized model of dyad **4** show that the frontier orbitals are localized either on the Bodipy (HOMO−1 and LUMO) or on the porphyrin (HOMO and LUMO+1) parts of the molecule and do not possess any bridge character.[39] On this basis, in addition to the UV−Vis absorption data of the dyads, we expect no significant orbital interactions between the two chromophores and the bridging units in **4** and **5**. Furthermore, the spectroscopic data measured for the model compounds **1**, **2**, and **3** allowed us to estimate the Dexter overlap integrals in **4** and **5** at $J_{D/4} = 0.21\ eV^{-1}$ and $J_{D/5} = 0.12\ eV^{-1}$, respectively. According to eq 1, the electronic interaction factors for **4** and **5** should be $H_4 = 31\ cm^{-1}$ and $H_5 = 35\ cm^{-1}$ to reproduce the experimentally measured energy transfer rates of $k_4 = 2.9 \times 10^{10}\ s^{-1}$ and $k_5 = 2.2 \times 10^{10}\ s^{-1}$. Such values seem to be too high considering the poor orbital interactions between the constituent chromophores in **4** and **5**.[40−42] Therefore, photoinduced energy transfer by the Dexter mechanism is considered highly unlikely for dyads **4** and **5**.

The spectroscopic overlap integrals for Coulombic Förster-type Bodipy to porphyrin energy transfer for **4** and **5** were estimated at $J_{F/4} = 8.6 \times 10^{-14}\ cm^6$ and $J_{F/5} = 5.7 \times 10^{-14}\ cm^6$ using the experimentally determined spectroscopic parameters of the model compounds **1**, **2**, and **3**. The corresponding critical radii for **4** and **5** were found to be $R_{c/4} = 42.3$ Å and $R_{c/5} = 39.5$ Å assuming a dynamically averaged orientation ($\kappa^2 = 2/3$)[37,43] of the constituent chromophores in the dyads. Such an assumption is valid given the high degree of rotational freedom and flexibility of the bridging unit. According to eq 3, the interchromophoric distances in **4** and **5** are estimated at $r_4 = 20.1$ Å and $r_5 = 19.6$ Å using the measured energy transfer rates of $k_4 = 2.9 \times 10^{10}\ s^{-1}$ and $k_5 = 2.2 \times 10^{10}\ s^{-1}$. The results of a geometry optimization on a model of dyad **4** (Figure 11) show that the interchromophoric distance (taken as the distance from the center of the porphyrin ring to the boron atom of the Bodipy moiety) in the minimum energy conformation, where the bridging unit adopts a fully extended configuration, is 22.2 Å. However, the bridging

dx.doi.org/10.1021/ic201052k |*Inorg. Chem.* 2011, 50, 8926–8936

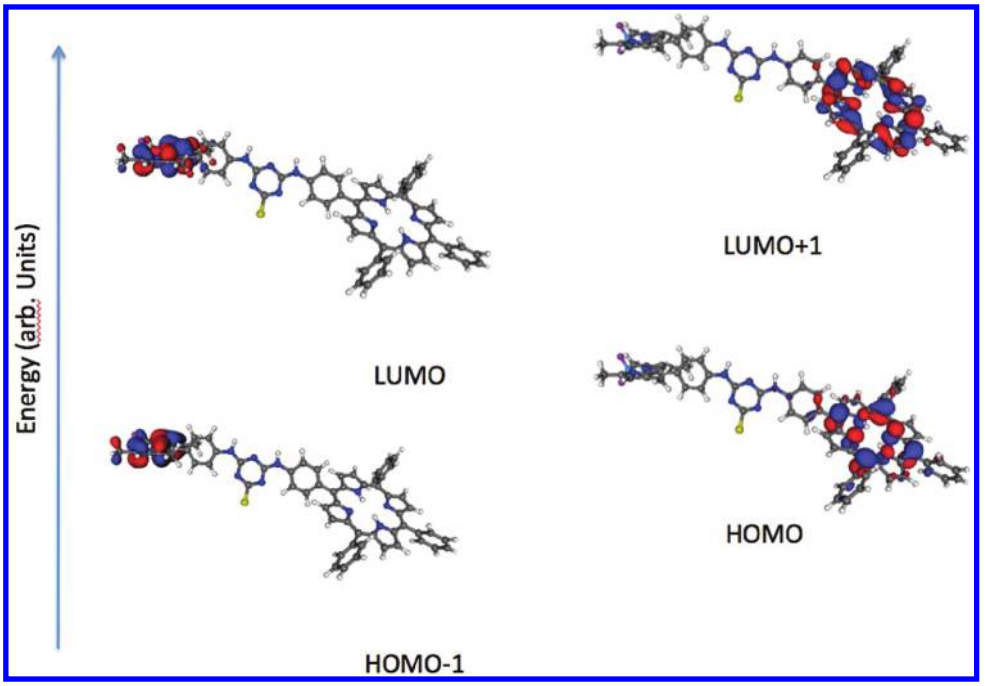

Figure 10. Frontier orbitals of dyad **4**.

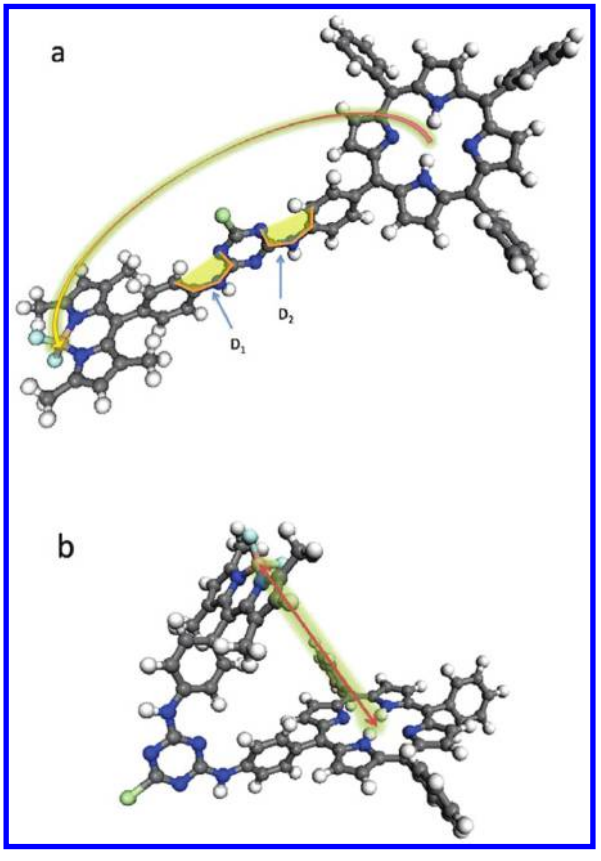

Figure 11. Optimized molecular geometries of the two lowest energy conformations of **4** predicted from DFT calculations. D1 and D2 (yellow line) correspond to the dihedral angles that were varied during semiempirical calculations. Carbon, nitrogen, chlorine, boron, fluorine, and hydrogen atoms are shown in gray, blue, green, purple, cyan, and white, respectively.

unit can easily undergo conformational rearrangements due to free rotation about the dihedral angles D1 and D2 (Figure 11). For instance, as shown in Figure 9b, a minimum configuration is found at which the interchromophoric distance is 11.2 Å. Consequently, in solution, dyads **4** and **5** adopt a variety of conformations between the two extremes shown in Figure 11, probably favoring the more extended conformations of the bridging unit. Therefore, the measured energy transfer rates in **4** and **5** fit well to the Förster mechanism and reflect the flexibility of the bridging unit.

EXPERIMENTAL SECTION

Photophysical Measurements. UV−Vis absorption spectra were measured on a Shimadzu UV-1700 spectrophotometer using 10 mm path-length cuvettes. The emission spectra were measured on a JASCO FP-6500 fluorescence spectrophotometer equipped with a red-sensitive WRE-343 photomultiplier tube (wavelength range 200−850 nm). Quantum yields were determined from corrected emission spectra following the standard methods[15] using *meso*-tetraphenylporphyrin (TPP) ($\Phi = 0.11$ in toluene[16]) or zinc *meso*-tetraphenylporphyrin (ZnTPP) ($\Phi = 0.03$ in toluene[16]) as standards. Emission lifetimes were determined by the time-correlated single-photon counting technique using an Edinburgh Instruments mini-tau lifetime spectrophotometer equipped with an EPL 405 pulsed diode laser at 406.0 nm with a pulse width of 71.52 ps and a pulse period of 200 ns and a high-speed red-sensitive photomultiplier tube (H5773-04) as detector. Calculations of Förster and Dexter spectral overlap integrals and critical radii for Förster energy transfer were performed using the photochemCAD computer program version 2.1.[17] Femtosecond transient absorption studies were performed with 420 and 387 nm laser pulses (1 kHz, 150 fs pulse width) from an amplified Ti:Sapphire laser system (Clark-MXR, Inc. CPA 2101); the laser energy was 200 nJ.

Computational Details. We used quantum chemistry semiempirical calculations to locate the minimum energy conformations of the molecule by performing a grid calculation in which we varied

dx.doi.org/10.1021/ic201052k |*Inorg. Chem.* 2011, 50, 8926–8936

simultaneously two coordinates corresponding to the dihedral angles D1 and D2 (Figure 11). We used these methods in order to extract important qualitative relations in much shorter computational times than any ab initio method. These calculations were done at the PM6[18,19] semiempirical level with the MOPAC2009,[20] version 9.259W, package. Calculations resulted in formation of a 2D contour plot of the varied coordinates with respect to the total energy, from which we were able to find the two lowest conformations in energy. The latest conformations were further explored by performing more sophisticated quantum chemistry calculations within the framework of density functional theory (DFT). Density functional theory in the resolution of identity (RI) approximation[21] was applied in our calculations. The B-P86[22] exchange-correlation functional along with the def2-SVP[23] basis set (with the corresponding auxiliary basis set for the RI approximation) was used. All structures were optimized without any symmetry constraints, and the optimized minimum-energy structures were verified as stationary points on the potential energy surface by performing numerical harmonic vibrational frequency calculation. DFT calculations were performed with the TURBOMOLE program.[24]

Materials. **$TPPNH_2$**[25] and **$BDPNH_2$**[26] (Scheme 1) were prepared using published procedures. All other chemicals and solvents were purchased from the usual commercial sources and used as received unless otherwise stated. Tetrahydrofuran was freshly distilled from Na/benzophenone, and anhydrous K_2CO_3 was ground in a mortar and pestle and dried in an oven at 150 °C overnight prior to use.

5-[4-(4,6-Dichloro-1,3,5-triazin-2-ylamino)phenyl]-10,15,20-triphenyl-porphyrin (2).[27]. A 0.070 g (0.11 mmol) amount of **$TPPNH_2$** was added to a suspension of 0.076 g (0.55 mmol) of anhydrous K_2CO_3 in dry THF (10 mL). The mixture was stirred in an ice bath at 0 °C under an atmosphere of dry nitrogen for ∼5 min before adding 0.024 g (0.13 mmol) of cyanuric chloride. The resulting mixture was allowed to slowly reach room temperature while being stirred. Completion of the reaction was followed and confirmed by TLC (silica gel, dichloromethane/hexanes 4:1). A stream of nitrogen removed the solvent, the solid residue was subjected to column chromatography (silica gel, dichloromethane/hexanes 4:1), and the principal purple band was collected. The desired product was isolated as a purple powder. Yield: 0.072 g (80%). ^{1}H NMR (500 MHz, $CDCl_3$): δ 8.87 (m, 8H), 8.23 (m, 8H), 7.88 (d, J = 8.5 Hz, 2H), 7.82−7.74 (m, 10H), −2.74 ppm (s, 2H). ^{13}C NMR (75 MHz, $CDCl_3$): δ 164.2, 142.1, 139.6, 135.6, 135.3, 134.6, 131.3, 127.8, 126.7, 120.4, 120.3, 119.1, 118.7 ppm. UV−Vis (CH_2Cl_2): λ_{max} (ε, mol^{-1} dm^3 cm^{-1}) 418 (478 000), 514 (19 000), 549 (9000), 589 (6000), 645 nm (4500). HRMS (MALDI-TOF): m/z calcd for $C_{47}H_{30}Cl_2N_8$ + H^+: 777.2049 [M + H]$^+$. Found: 777.2061. Anal. Calcd for $C_{47}H_{30}Cl_2N_8$: C, 72.59; H, 3.89; N, 14.41. Found: C, 72.68; H, 3.65; N, 14.55.

{5-[4-(4,6-Dichloro-1,3,5-triazin-2-ylamino)phenyl]-10,-15,20-triphenyl-porphyrinato}zinc(II) (3). A 0.020 g amount of **2** (0.025 mmol) was dissolved in 3:1 dichloromethane/methanol (10 mL), and 0.055 g (0.25 mmol) of $Zn(CH_3COO)_2 \cdot 2H_2O$ was added. The resulting mixture was stirred at room temperature overnight. At the end of the reaction the solvent was removed in a rotary evaporator and the resulting residue was partitioned between dichloromethane (5 mL) and water (5 mL). The organic layer was further washed with 5 mL of water and dried with Na_2SO_4. The solvent was removed, and the residue was passed through a short column of silica eluting with dichloromethane. The desired product was isolated as red-purple powder. Yield: 0.018 g (84%). ^{1}H NMR (500 MHz, $CDCl_3$): δ ^{1}H NMR (500 MHz, $CDCl_3$/1% pyridine-d_5): δ 8.78 (m, 8H), 8.11 (m, 8H), 7.73 (s br, 2H), 7.57 ppm (m, 10H). ^{13}C NMR (75 MHz, $CDCl_3$/1% pyridine-d_5): δ 149.7, 142.9, 136.0, 134.5, 131.8, 127.2, 126.4, 120.6, 119.6 ppm. UV−Vis (CH_2Cl_2): λ_{max} (ε, mol^{-1} dm^3 cm^{-1}) 419 (585 000), 542 (20 400), 583 nm (6000). HRMS (MALDI-TOF): m/z calcd for $C_{47}H_{28}Cl_2N_8Zn$ + H^+: 839.1184 [M + H]$^+$. Found: 839.1172. Anal. Calcd for $C_{47}H_{28}Cl_2N_8Zn$: C, 67.12; H, 3.36; N, 13.32. Found: C, 67.24; H, 3.45; N, 13.21.

4,4-Difluoro-8-[4-(4,6-dichloro-1,3,5-triazin-2ylamino)-phenyl]-1,3,5,7-tetramethyl-4-bora-3a,4a-diaza-*s*-indacene (1). A 0.085 g (0.25 mmol) amount of **$BDPNH_2$** was added to a suspension of 0.173 g (1.25 mmol) of anhydrous K_2CO_3 in dry THF (10 mL). The mixture was stirred in an ice bath at 0 °C under an atmosphere of dry nitrogen for ∼5 min before adding 0.055 g (0.3 mmol) of cyanuric chloride. The resulting mixture was allowed to slowly reach room temperature while being stirred. Completion of the reaction was confirmed by TLC (silica gel, dichloromethane/hexanes 4:1). A stream of nitrogen removed the solvent, the solid residue was subjected to column chromatography (silica gel, dichloromethane/hexanes 4:1), and the principal bright orange band was collected. The desired product was isolated as an orange powder. Yield: 0.080 g (64%). ^{1}H NMR (500 MHz, $CDCl_3$): δ 7.76 (d, J = 8.5 Hz, 2H), 7.68 (s, 1H), 7.33 (d, J = 8.5 Hz, 2H), 5.99 (s, 2H), 2.56 (s, 6H), 1.43 ppm (s, 6H). ^{13}C NMR (75 MHz, $CDCl_3$): δ 164.1, 156.0, 143.1, 140.6, 137.0, 132.2, 131.6, 129.4, 121.5, 121.2, 14.8 ppm. UV−Vis(CH_2Cl_2): λ_{max} (ε, mol^{-1} dm^3 cm^{-1}) 277 (33 000), 342 (9400), 502 nm (75 600). HRMS (MALDI-TOF): m/z calcd for $C_{22}H_{19}BCl_2F_2N_6$ + H^+: 487.1188 [M + H]$^+$. Found: 487.1173. Anal. Calcd for $C_{22}H_{19}BCl_2F_2N_6$: C, 54.24; H, 3.93; N, 17.25. Found: C, 54.11; H, 3.75; N, 17.41.

5-{4-[4-Chloro-6-(aminophenyl-4-(4,4-difluoro-8-(1,3,5,7-tetramethyl-4-bora-3a,4a-diaza-*s*-indacene)))-1,3,5-triazin-2-ylamino]phenyl}-10,15,20-triphenylporphyrin (4). A 0.055 g amount of **2** (0.071 mmol) and 0.024 g (0.071 mmol) of **$BDPNH_2$** were added to a suspension of 0.039 g (0.284 mmol) of anhydrous K_2CO_3 in dry THF (10 mL) in a Schlenck tube under an atmosphere of dry nitrogen. The tube was sealed, and the mixture was stirred at 60 °C for 24 h. At the end of the reaction the mixture was filtered to remove the K_2CO_3 and the solvent was removed in a rotary evaporator. The crude product was subjected to column chromatography (silica gel, dichloromethane), and the principal orange-red band was collected. The product was isolated as a red-purple powder. Yield: 0.048 g (61%). ^{1}H NMR (500 MHz, $CDCl_3$): δ 8.85 (s, 8H), 8.22 (s, 8H), 7.97 (s, 2H), 7.76 (s, 12H), 7.58 (s, 1H), 7.26 (s, 2H), 5.99 (s br, 1H), 5.65 (s br, 1H), 2.57 (s br, 3H), 2.27 (s br, 3H), 1.41 (s, 6H), −2.76 ppm (s, 2H). ^{13}C NMR (75 MHz, $CDCl_3$): δ 164.5, 155.6, 143.0, 142.3, 138.6, 137.1, 135.2, 134.7, 131.6, 129.0, 127.9, 126.9, 121.4, 120.5, 120.4, 118.9, 14.8, 14.6 ppm. UV−Vis (CH_2Cl_2): λ_{max} (ε, mol^{-1} dm^3 cm^{-1}) 419 (419 000), 500 (74 800), 550 (8300), 589 (5200), 645 nm (4200). HRMS (MALDI-TOF): m/z calcd for $C_{66}H_{49}BClF_2N_{11}$ + H^+: 1080.4000 [M + H]$^+$. Found: 1080.4012. Anal. Calcd for $C_{66}H_{49}BClF_2N_{11}$: C, 73.37; H, 4.57; N, 14.26. Found: C, 73.28; H, 4.67; N, 14.12.

{5-[4-[4-Chloro-6-(aminophenyl-4-(4,4-difluoro-8-(1,3,5,7-tetramethyl-4-bora-3a,4a-diaza-*s*-indacene)))-1,3,5-triazin-2-ylamino]phenyl]-10,15,20-triphenylporphyrinato}zinc(II) (5). A 0.020 g (0.018 mmol) amount of **4** was dissolved in 3:1 dichloromethane/methanol (10 mL), and 0.040 g (0.180 mmol) of $Zn(CH_3COO)_2 \cdot 2H_2O$ was added. The resulting mixture was stirred at room temperature overnight. At the end of the reaction the solvent was removed in a rotary evaporator and the resulting residue was partitioned between dichloromethane (5 mL) and water (5 mL). The organic layer was further washed with 5 mL of water and dried with Na_2SO_4. The solvent was removed, and the residue was passed through a short column of silica eluting with dichloromethane. The desired product was isolated as a red-purple powder. Yield: 0.016 g (78%). ^{1}H NMR (300 MHz, $CDCl_3$): δ 8.95 (s, 8H), 8.22 (m, 8H), 7.96 (d, J = 8.1 Hz, 2H), 7.77 (m, 12H), 7.59 (s br, 1H), 7.23 (m, 2H), 5.96 (s br, 1H), 5.67 (s br, 1H), 2.55 (s br, 3H), 2.25 (s br, 3H), 1.42 ppm (m, 6H). ^{13}C NMR (75 MHz, $CDCl_3$): δ 164.6, 155.6, 150.4, 142.9, 138.1, 136.9, 135.0, 134.6, 132.2, 129.0, 127.7, 126.7, 121.3, 118.9, 14.8 ppm. UV−Vis (CH_2Cl_2): λ_{max} (ε, mol^{-1}

$dm^3\ cm^{-1}$) 420 (434 000), 500 (75 300), 546 (21 500), 583 nm (7200). HRMS (MALDI-TOF): *m/z* calcd for $C_{66}H_{47}BClF_2N_{11}Zn + H^+$: 1142.3135 $[M + H]^+$. Found: 1142.3148. Anal. Calcd for $C_{66}H_{47}BClF_2N_{11}Zn$: C, 69.30; H, 4.14; N, 13.47. Found: C, 69.19; H, 4.27; N, 13.67.

CONCLUSIONS

We report the synthesis of dyads **4** and **5** which combine the Bodipy chromophore with either a free-base or a Zn porphyrin moiety linked to eachother via a cyanuric chloride bridge. The photophysical behavior of **4** and **5** was studied by UV−Vis absorption and emission spectroscopy, cyclic voltammetry and femptosecond transient absorption spectroscopy. Comparison of the absorption spectra and cyclic voltammograms of dyads **4** and **5** with those of their model compounds **1**, **2**, and **3** shows that the spectroscopic and electrochemical properties of the constituent chromophores are essentially retained in the dyads, indicating negligible interaction between them in the ground state. In contrast, luminescence and transient absorption experiments show that excitation of the Bodipy unit in **4** and **5** into its first singlet excited state results in rapid Bodipy to porphyrin energy transfer (rates, $k_4 = 2.9 \times 10^{10}\ s^{-1}$ and $k_5 = 2.2 \times 10^{10}\ s^{-1}$ for **4** and **5**, respectively), generating the first porphyrin-based singlet excited state. The porphyrin-based singlet excited states give rise to fluorescence or undergo intersystem crossing to the corresponding triplet states. Therefore, the Bodipy unit increases the light-harvesting potential of the porphyrin chromophore excited state, and functionalized derivatives of **4** and **5** could be excellent precursors for further substitution and/or excellent sensitizers in DSSCs.

ASSOCIATED CONTENT

Supporting Information. Complementary data of differential absorption spectra and their time-absorption profiles, as well as the ^{1}H-NMR, ^{13}C-NMR of the title compounds **1**, **2**, **3**, **4**, and **5**. This material is available free of charge via the Internet at http://pubs.acs.org.

DEDICATION

[⊥]This work is dedicated to the memory of our colleague and friend Nikos Manoussakis.

AUTHOR INFORMATION

Corresponding Author

*E-mail: marius.reglier@univ-cezanne.fr (M.R.); dirk.guldi@chemie.uni-erlangen.de (D.M.G.); coutsole@chemistry.uoc.gr (A.G.C.).

ACKNOWLEDGMENT

The European Commission funded this research by FP7-REGPOT-2008-1, Project BIOSOLENUTI No 229927, Heraklitos grant from Ministry of Education, and GSRT. In addition, financial support from the DFG (Cluster of Excellence and SFB 583) and the BMBF is greatly acknowledged.

REFERENCES

(1) Ward, M. D. *Chem. Soc. Rev.* **1997**, *26*, 365–375.
(2) Ward, M. D. *Chem. Soc. Rev.* **1995**, *24*, 121–134.
(3) Balzani, V.; Bergamini, G.; Ceroni, P. *Coord. Chem. Rev.* **2008**, *252*, 2456–2469.
(4) Campbell, W. M.; Burrell, A. K.; Officer, D. L.; Jolley, K. W. *Coord. Chem. Rev.* **2004**, *248*, 1363–1379.
(5) Lo, C. F.; Hsu, S. J.; Wang, C. L.; Cheng, Y. H.; Lu, H. P.; Diau, E. W. G.; Lin, C. Y. *J. Phys. Chem. C* **2010**, *114*, 12018–12023.
(6) Jensen, R. A.; Van Ryswyk, H.; She, C. X.; Szarko, J. M.; Chen, L. X.; Hupp, J. T. *Langmuir* **2010**, *26*, 1401–1404.
(7) Kadish, K. M.; Smith, K. M.; Guilard, R. *The porphyrin handbook*; Academic: San Diego, London, 2000.
(8) (a) Maligaspe, E.; Kumpulainen, T.; Subbaiyan, N. K.; Zandler, M. E.; Lemmetyinen, H.; Tkachenko, N. V.; D'Souza, F. *Phys. Chem. Chem. Phys.* **2010**, *12*, 7434–7444. (b) Rio, Y.; Seitz, W.; Gouloumis, A.; Vazquez, P.; Sessler, J. L.; Guldi, D. M.; Torres, T. *Chem.—Eur. J.* **2010**, *16*, 1929–1940.
(9) Lee, C. Y.; Hupp, J. T. *Langmuir* **2010**, *26*, 3760–3765.
(10) Carofiglio, T.; Varotto, A.; Tonellato, U. *J. Org. Chem.* **2004**, *69*, 8121–8124.
(11) Ichihara, K.; Naruta, Y. *Chem. Lett.* **1995**, 631–632.
(12) Carofiglio, T.; Lubian, E.; Menegazzo, I.; Saielli, G.; Varotto, A. *J. Org. Chem.* **2009**, *74*, 9034–9043.
(13) Tao, M. L.; Liu, D. Z.; Zhang, M. H.; Zhou, X. Q. *Acta Chim. Sin.* **2008**, *66*, 1252–1258.
(14) Carofiglio, T.; Schlorlin, M.; Tonellato, U. *J. Porphyrins Phthalocyanines* **2007**, *11*, 749–754.
(15) Demas, J. N.; Crosby, G. A. *J. Phys. Chem.* **1971**, *75*, 991–&.
(16) Seybold, P. G.; Gouterman, M. *J. Mol. Spectrosc.* **1969**, *31*, 1–13.
(17) Du, H.; Fuh, R. C. A.; Li, J. Z.; Corkan, L. A.; Lindsey, J. S. *Photochem. Photobiol.* **1998**, *68*, 141–142.
(18) Stewart, J. J. P. *J. Mol. Model.* **2007**, *13*, 1173–1213.
(19) Stewart, J. J. P. *J. Mol. Model.* **2008**, *14*, 499–535.
(20) In *Computational Chemistry*; Stewart, J. J. P., Ed.; 2009.
(21) Weigend, F.; Haser, M.; Patzelt, H.; Ahlrichs, R. *Chem. Phys. Lett.* **1998**, *294*, 143–152.
(22) Becke, A. D. *Phys. Rev. A* **1988**, *38*, 3098–3100.
(23) Weigend, F.; Ahlrichs, R. *Phys. Chem. Chem. Phys.* **2005**, *7*, 3297–3305.
(24) Ahlrichs, R.; Bar, M.; Haser, M.; Horn, H.; Kolmel, C. *Chem. Phys. Lett.* **1989**, *162*, 165–169.
(25) Luguya, R.; Jaquinod, L.; Fronczek, F. R.; Vicente, A. G. H.; Smith, K. M. *Tetrahedron* **2004**, *60*, 2757–2763.
(26) Imahori, H.; Norieda, H.; Yamada, H.; Nishimura, Y.; Yamazaki, I.; Sakata, Y.; Fukuzumi, S. *J. Am. Chem. Soc.* **2001**, *123*, 100–110.
(27) Ghiggino, K. P.; Hutchison, J. A.; Langford, S. J.; Latter, M. J.; Takezaki, M. *J. Phys. Org. Chem.* **2006**, *19*, 491–494.
(28) Ziessel, R.; Allen, B. D.; Rewinska, D. B.; Harriman, A. *Chem.—Eur. J.* **2009**, *15*, 7382–7393.
(29) Burghart, A.; Kim, H. J.; Welch, M. B.; Thoresen, L. H.; Reibenspies, J.; Burgess, K.; Bergstrom, F.; Johansson, L. B. A. *J. Org. Chem.* **1999**, *64*, 7813–7819.
(30) Karolin, J.; Johansson, L. B. A.; Strandberg, L.; Ny, T. *J. Am. Chem. Soc.* **1994**, *116*, 7801–7806.
(31) Guldi, D. M. *Chem. Soc. Rev.* **2002**, *31*, 22–36.
(32) D'Souza, F.; Smith, P. M.; Zandler, M. E.; McCarty, A. L.; Itou, M.; Araki, Y.; Ito, O. *J. Am. Chem. Soc.* **2004**, *126*, 7898–7907.
(33) Li, F. R.; Yang, S. I.; Ciringh, Y. Z.; Seth, J.; Martin, C. H.; Singh, D. L.; Kim, D. H.; Birge, R. R.; Bocian, D. F.; Holten, D.; Lindsey, J. S. *J. Am. Chem. Soc.* **1998**, *120*, 10001–10017.
(34) Lazarides, T.; McCormick, T. M.; Wilson, K. C.; Lee, S.; McCamant, D. W.; Eisenberg, R. *J. Am. Chem. Soc.* **2011**, *133*, 350–364.
(35) Darwent, J. R.; Douglas, P.; Harriman, A.; Porter, G.; Richoux, M. C. *Coord. Chem. Rev.* **1982**, *44*, 83–126.
(36) Dexter, D. L. *J. Chem. Phys.* **1953**, *21*, 836–850.
(37) Förster, T. *Discuss. Faraday Soc.* **1959**, *27*, 7–17.
(38) Chiorboli, C.; Indelli, M. T.; Scandola, F. *Top. Curr. Chem.* **2005**, *257*, 63–102.

(39) Maligaspe, E.; Kumpulainen, T.; Lemmetyinen, H.; Tkachenko, N. V.; Subbaiyan, N. K.; Zandler, M. E.; D'Souza, F. *J. Phys. Chem. A* **2010**, *114*, 268–277.
(40) Flamigni, L.; Talarico, A. M.; Barigelletti, F.; Johnston, M. R. *Photochem. Photobiol. Sci.* **2002**, *1*, 190–197.
(41) Otsuki, J.; Harada, K.; Toyama, K.; Hirose, Y.; Araki, K.; Seno, M.; Takatera, K.; Watanabe, T. *Chem. Commun.* **1998**, 1515–1516.
(42) Closs, G. L.; Johnson, M. D.; Miller, J. R.; Piotrowiak, P. *J. Am. Chem. Soc.* **1989**, *111*, 3751–3753.
(43) Lakowicz, J. R. *Principles of Fluorescence Spectroscopy*; Kluwer/Plenum: New York, 1999.